Two-Directional Photoinduced Electron Transfer in a Trichromophoric System

Sigrid Depaemelaere and Frans C. De Schryver*

Laboratory of Molecular Dynamics and Spectroscopy, KU Leuven, Celestijnenlaan 200F, B-3001 Heverlee, Belgium

Jan W. Verhoeven

Laboratory of Organic Chemistry, University of Amsterdam, Nieuwe Achtergracht 129, 1018 WS Amsterdam, The Netherlands

Received: October 31, 1997; In Final Form: January 13, 1998

Competition between electron transfer via a through σ-bond and a through π-bond mechanism has been studied in 1-(4-cyanophenyl)-4-(cyanomethylene)piperidine. In this trichromophoric system designed in a configuration acceptor−donor−acceptor, where the donor chromophore is part of the initially excited state, electron transfer occurs in two directions. The results of the single-photon-timing measurements indicate that, in both diethyl ether and acetonitrile, two charge-transfer states, a σCT and a πCT state, are formed, by transferring the electron through the σ- or π-bonds, respectively. Information on the excited-state kinetics is obtained by means of global compartmental analysis of the fluorescence decay surface in acetonitrile. Both the σCT and πCT state are formed immediately upon excitation, within the time resolution of the experimental setup, and an electron exchange between the two polar states occurs at least in one direction.

Introduction

In the last decades photoinduced intramolecular electron transfer has been a subject of extensive study. The basic unit in which electron transfer can be studied comprises a single electron donor and a single electron acceptor. To obtain a long-lived charge separation, bichromophoric systems have been extended to molecules with three or more chromophores in which stepwise electron transfer takes place.[1−12] A trichromophoric system comprising one donor and two acceptor chromophores can also be used to compare directly two different electron-transfer pathways. In a system designed in a configuration A1−D−A2, if the donor chromophore is part of the initially excited state, electron transfer can occur in two directions depending on the factors that influence the electron-transfer mechanism.

We synthesized and studied a range of compounds with an ADA configuration in which one of the acceptors was varied.[13] Depending on the strength of this acceptor, the electron-transfer direction can be differed from exclusively to the first acceptor to exclusively to the second acceptor if its strength is increased. In this paper, we focus on one compound in this series, 1-(4-cyanophenyl)-4-(cyanomethylene)piperidine (PCN2), which shows an intermediate and specific behavior. In this compound, the amino part of the molecule acts as a one-electron donor and is directly coupled via a phenyl (π-system) bridge to a cyano group. This A1−D part of the molecule resembles the extensively studied compound dimethylaminobenzonitrile. It is known that this class of compounds exhibits dual fluorescence from an initially excited and a charge-separated state. The second acceptor is a monocyanomethylene group, which is connected via a rigid spacer of three σ-bonds to the amino donor. In this D−A2 part of the compound D and A are separated by a rigid spacer over a distance larger than the sum of the van der Waals radii. Yet, there is still coupling between D and A as a consequence of their interaction with the σ-bonds of the connecting spacer. Due to this through σ-bond interaction, electron transfer can still occur over these large distances. The D−A2 part of the molecule resembles the through σ-bond bichromophoric compounds studied by Hermant et al.[15] By combining the two systems in one molecule, a trichromophoric system is created in which electron transfer can occur in two competing directions, via a through π-bond or a through σ-bond mechanism, respectively. A kinetic scheme is proposed and information on the excited-state kinetics is obtained by means of global compartmental analysis of the fluorescence decay surface in acetonitrile.

Experimental Section

Synthesis of PCN2 and PIPBN. 1-(4-Cyanophenyl)-4-(cyanomethylene)piperidine (compound PCN2) has been synthesized in a three-step procedure. First the compound 1-(4-cyanophenyl)-4-piperidone was synthesized in two steps according to literature procedures.[14] Treatment of 4-fluorobenzonitrile with 1,4-dioxa-8-azaspiro[4,5]decane in refluxing acetonitrile containing anhydrous potassium carbonate gave 1-(4-cyanophenyl)-4-piperidone ethylene acetal. Mild acidic hydrolysis (10% sulfuric acid/tetrahydrofuran/3-4 days/25 °C) provided 1-(4-cyanophenyl)-4-piperidone. PCN2 then was synthesized via a Wittig−Horner reaction analogous to similar compounds.[15] A solution of 7 mmol of the ketone and 9 mmol of the diethyl cyanomethylenephosphonate in 20 mL of dry tetrahydrofuran under inert atmosphere was cooled in ice. A 0.3 g sample of NaH (80% suspension in paraffinic oil) was added gradually. The ice bath was removed, and the reaction mixture was stirred for an additional period. The reaction was followed on TLC. After addition of water and extraction with dichloromethane, the collected organic layers were dried on $MgSO_4$ and evaporated to dryness. The crude product was purified by repeated

* Fax: +32 16 32 79 89. E-mail: Frans.Deschryver@chem.kuleuven.ac.be.

S1089-5639(98)00039-5 CCC: $15.00
Published on Web 02/27/1998

SCHEME 1: Schematic Picture of an Intramolecular Bicompartmental System

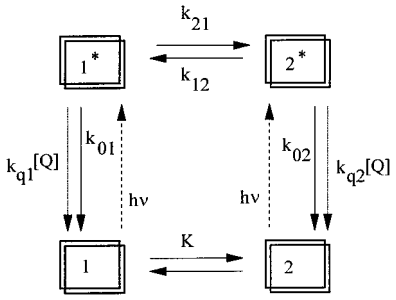

recrystallization in methanol: ^{1}H NMR (400 MHz, $CDCl_3$) δ 7.5 (d, 2H), δ 6.9 (d, 2H), δ 5.2 (s, 1H), δ 3.5 (m, 4H), δ 2.6 (t, 2H), δ 2.5 (t, 2H).

The model compound 4-piperidinobenzonitrile (PIPBN) was synthesized in an analogous way as 1-(4-cyanophenyl)-4-piperidone ethylene acetal from 4-fluorobenzonitrile and piperidine: ^{1}H NMR (400 MHz, $CDCl_3$) δ 7.5 (dd, 2H), δ 6.8 (dd, 2H), δ 3.3 (t, 4H), δ 1.7 (m, 6H).

Instrumentation. Absorption spectra were recorded on a Perkin-Elmer Lambda 6 UV/vis spectrophotometer. Corrected fluorescence spectra were measured using a SPEX fluorolog 1691 spectrophotometer. The fluorescence decay curves were obtained by the single-photon-timing (spt) technique described before.[16,17] The fluorescence light was detected by a cooled microchannel plate (Hamamatsu R3809U) after passing a polarizer set at magic angle and a monochromator. The width of the instrumental response function measured with a LUDOX scattering solution is smaller than 50 ps. The excitation wavelength was 295 nm, and the fluorescence decay curves, collected in 511 channels of the multichannel analyzer, contained a minimum of 10 000 peak counts. The fluorescence decays were analyzed by the global analysis program, using the reference deconvolution method[18−21] with POPOP (*p*-bis[2-(5-phenyloxazoyl)benzene], τ = 1.1 ns) and PPO (2,5-diphenyloxazole, τ = 1.4 ns) as reference compounds. The fluorescence decays of PIPBN were analyzed globally over different emission wavelengths: in isooctane between 340 and 400 nm at a time increment of 35 ps/ch, in diethyl ether between 340 and 440 nm at 30 ps/ch, and in acetonitrile between 360 and 600 nm at 23 ps/ch. The fluorescence decays of PCN2 were analyzed globally over different emission wavelengths: in isooctane between 340 and 400 nm at a time increment of 25 ps/ch, in diethyl ether between 370 and 500 nm at 35 and 18 ps/ch, and in acetonitrile between 380 and 560 nm at 59 and 117 ps/ch.

Sample Preparation. Samples for stationary and time-resolved fluorescence measurements were degassed by several freeze−pump−thaw cycles. The solvents used were of spectroscopic grade and were used as received. NaI 99.99+% (Aldrich) was used as fluorescence quencher.

Parameter Estimation. The fittings of the models to data were performed on a IBM 6000 RISC using the previously described analysis program.[22] For intramolecular two-state excited-state processes with added quencher, the global fitting parameters are k_{01}, k_{21}, k_{q1}, k_{02}, k_{12}, and k_{q2}, the normalized absorbance $\tilde{b}_1(\lambda^{ex})$, and the normalized spectral emission weighting factor $\tilde{c}_1(\lambda^{em})$[20] (Scheme 1). The fitting parameter values were estimated by minimizing the global reduced χ_g^2,

$$\chi_g^2 = \sum_l^q \sum_i w_{li}(y^o_{li} - y^c_{li})^2/\nu \qquad (1)$$

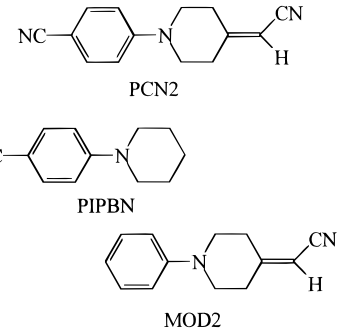

Figure 1. Compounds used in the study: the trichromophore PCN2 and the model compounds PIPBN and MOD2.

where the index l sums over q experiments and the index i sums over the appropriate channel limits for each individual experiment. y^o_{li} and y^c_{li} denote respectively the observed (synthetic) and calculated (fitted) values corresponding to the ith channel of the lth experiment, w_{li} is the corresponding statistical weight, and ν represents the number of degrees of freedom for the entire multidimensional fluorescence decay surface. The numerical statistical tests incorporated the calculation of χ_g^2 and its corresponding $Z_{\chi_g^2}$:

$$Z_{\chi_g^2} = \left(\frac{1}{2}\nu\right)^{1/2}(\chi_g^2 - 1) \qquad (2)$$

Using $Z_{\chi_g^2}$, the goodness of the fit of analyses with different ν can be readily compared. The fit was considered to be good when the global $Z_{\chi_g^2} \leq 10$ over the entire data surface. The additional statistical criteria to judge the quality of the fits are described elsewhere.[17,23]

Results and Discussion

Trichromophoric System and Its Model Compounds. The structures of the trichromophoric compound PCN2 and the two model compounds are given in Figure 1. The model compounds are both bichromophoric systems in which electron transfer is possible only in one direction.

The model compound PIPBN resembles the A1−D part of the trichromophoric system. PIPBN belongs to the group of aminobenzonitriles. This class of compounds exhibits dual fluorescence from an initially excited and a charge-separated state.[24−27] Presently there is still some controversy about the nature of the charge-separated state and about the structural changes that accompany its formation.[26−44] The kinetic scheme for charge-transfer formation in aminobenzonitriles can be described by means of time-independent rate constants analogous to exciplex formation.[40,41,45] In some cases however a different behavior is reported for the decay in the short and long wavelength range.[45,46] The compound PIPBN shows dual fluorescence from an initially excited delocalized state (DE state) with partial charge-transfer character and a polar charge-separated state. Kinetic data for PIPBN are reported only at low temperature.[45,47,48] A biexponential decay was found with one decay time around 3 ns, while the other decreased when temperature increased from 320 ps at −105 °C[45] to 78 ps at −80 °C[48] in diethyl ether. Extrapolating to room temperature leads to a short decay time of around 6 ps.[49] At room temperature we could analyze all decay curves of PIPBN as a monoexponential decay with decay times of 2.74 ns in isooctane, 2.63 ns in diethyl ether, and 3.6 ns in acetonitrile. In acetonitrile, at short wavelengths, a second decay time of a few picoseconds could be detected but was too short to be measured accurately.

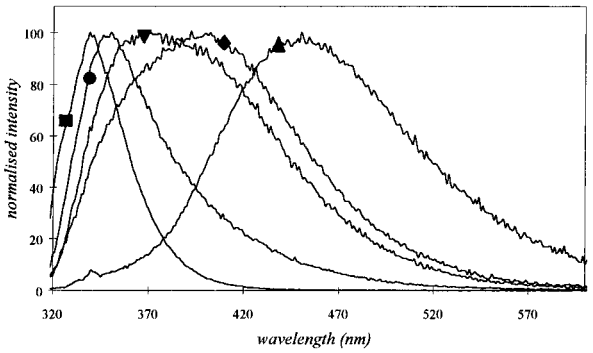

Figure 2. Normalized fluorescence spectra of PCN2 in (■) isooctane, (●) diethyl ether, (▼) butyl acetate, (♦) ethyl acetate, and (▲) acetonitrile.

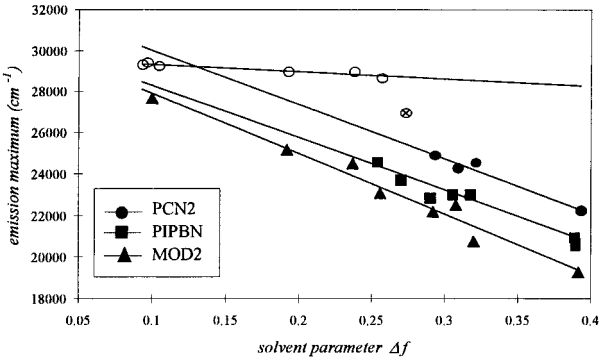

Figure 3. Lippert−Mataga plot: fluorescence maximum as a function of solvent polarity parameter Δf for PCN2, PIPBN, and MOD2. Maximum of the emission dominated by the initially excited state is indicated with open symbols. Maximum of the emission dominated by the charge-transfer state is indicated with filled symbols. The crossed symbol corresponds to an intermediate situation where both emission bands overlap considerably. Data for emission from the initially excited state for PIPBN are not indicated in the figure.

We conclude that, at room temperature, the two emissive states cannot be distinguished within the time resolution of the single-photon-timing setup. On the basis of the literature values for PIPBN and related compounds, we assume that the formation of the charge-separated state is fast in comparison with the decay of the delocalized excited state and that the rate of back reaction from the charge-separated state to the initially excited delocalized state decreases with increasing solvent polarity compared to the rate of formation. This causes an increase of charge-transfer fluorescence in the stationary emission spectrum.

The model compound MOD2 resembles the D−A2 part of the trichromophoric system. MOD2 is a bichromophoric compound in which donor and acceptor are separated by a rigid spacer over three σ-bonds, a distance larger than the sum of the van der Waals radii. Yet, there is still coupling between the donor and the acceptor as a consequence of their interaction with the σ-bonds of the connecting spacer. Due to this through σ-bond interaction, electron transfer can still occur over these large distances. The photophysical properties of MOD2 have been studied by Hermant et al.[15] The emission spectrum is strongly solvent dependent and consists of only one band, attributed to the charge-transfer state. The decay curves can be analyzed as a single exponential. It should be noted that the model system has a different donor capacity than the trichromophoric system owing to the absence of the cyano group. The donor capacity of the anilino part in the trichromophoric system is therefore about 2300 cm^{-1} lower than in the model compound. This value was obtained from the difference of the position of the maximum of the charge-transfer absorption band of the systems *N*-phenylpiperidine/tetrachloro-1,4-benzoquinone and 1-(4-cyanophenyl)piperidine/tetrachloro-1,4-benzoquinone. For the trichromophoric system, the charge-transfer state corresponding to the one in PIPBN will be denoted πCT, and the charge-transfer state corresponding to the one in MOD2 will be denoted σCT.

Steady-State Analysis. The absorption spectra of PIPBN and PCN2 are identical and consist of a nonstructured absorption band which is attributed to absorption of the cyanoaniline part of the molecule. The absorption maximum in isooctane is situated at 286 nm and is solvent dependent on solvent polarity due to the ground-state dipole moment. A solvent shift of 1300 cm^{-1} to longer wavelength is observed in changing the solvent from isooctane to acetonitrile.

The emission spectra of PCN2 in different solvents are reported in Figure 2. The position of the emission maximum is strongly dependent on solvent polarity. In isooctane the maximum is situated at 340 nm, in acetonitrile at 450 nm. Already in diethyl ether a broadening of the spectrum at the longer wavelength end is observed, indicating the appearance of charge-transfer emission. The spectra taken in solvents of intermediate polarity such as butyl acetate and ethyl acetate are broadened compared to other solvents, indicating an overlap of two different fluorescence bands.

The emission maximum of a dipolar excited state as a function of solvent polarity can be described by the following equation:[50−54]

$$\tilde{\nu}_{ct} = \tilde{\nu}^0_{ct} - \frac{2\mu^2}{4\pi\epsilon_0 hc\rho^3}\Delta f \qquad (3)$$

$$\Delta f = f - \frac{1}{2}f' = \frac{\epsilon - 1}{2\epsilon + 1} - \frac{n^2 - 1}{4n^2 + 2} \qquad (4)$$

$\tilde{\nu}_{ct}$ and $\tilde{\nu}^0_{ct}$ correspond respectively to the wavenumber of the emission maximum in a solvent with dielectric constant ϵ and refractive index n and the wavenumber of the emission maximum in the gas phase. ϵ_0, h, c, and ρ correspond to the permittivity of vacuum, the Planck constant, the velocity of light in vacuum, and the Onsager radius[55] for the solvent cavity. μ is the dipole moment of the excited state considering that the dipole moment of the ground state can be neglected.

As can be seen from Figure 3, when the emission maximum of PCN2 is plotted as a function of the solvent polarity parameter Δf, no linear relationship is observed. The data can be divided into two linear parts with a change in slope around butyl acetate. For the less polar solvents (from isooctane to diethyl ether) a linear relationship can be observed with a slope of -2900 cm^{-1}. Emission from the delocalized, initially excited, and less polar state (DE state) dominates. For solvents of high polarity (from ethyl acetate to acetonitrile) a straight line can be drawn with a slope of $-26\,400$ cm^{-1}. In these polar solvents emission from a highly polar state dominates. In the medium polar solvent butyl acetate, where a broad emission band is observed, the spectrum is a sum of both emissions and the apparent maximum lies intermediate. From these data it is clear that an emitting charge-separated state is formed in medium and polar solvents (diethyl ether to acetonitrile).

The question remains in which direction the electron will be transferred, causing the formation of a πCT or σCT state. The emission energy as a function of solvent polarity is compared with the data for the model compounds PIPBN and MOD2 (Figure 3). Comparing the slope of the relation for the polar state reveals an almost identical solvent stabilization for the polar

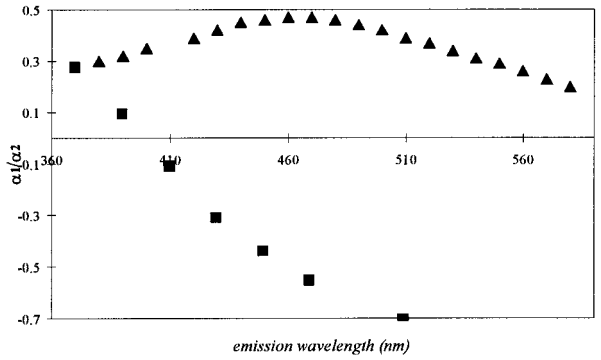

Figure 4. Ratio of the preexponential factors α_1/α_2 for PCN2 in diethyl ether (■) corresponding to $\tau_1 = 0.7$ ns and $\tau_2 = 3.1$ ns and in acetonitrile (▲) corresponding to $\tau_1 = 2.8$ ns and $\tau_2 = 11.6$ ns.

state of the three compounds. The relative energies of the emission maxima are comparable and give no information on the direction of electron transfer.

Fluorescence Decay Kinetics. Fluorescence decays were measured in isooctane, diethyl ether, and acetonitrile at different emission wavelengths. In isooctane the curves could globally be analyzed as a single-exponential decay with a decay time of 2.6 ns, comparable to PIPBN in the same solvent. This corresponds to the decay of the initially excited state. In diethyl ether and acetonitrile at least a biexponential function was necessary to describe the decay curves adequately with decay times of 0.7 and 3.1 ns in diethyl ether and 2.8 and 11.6 ns in acetonitrile. The ratios of the preexponential factors of the global analysis as a function of the emission wavelength are given in Figure 4.

Independently of whether a σCT or a πCT state is formed, on the basis of the data for the model compounds, we would expect a biexponential decay with one very short decay time (in the picosecond range), indicating a fast formation of the charge-transfer state from the initially excited state. This decay time might possibly be too small to be observed within the time resolution of the experimental setup. As the formation of the polar charge-transfer state occurs from the initially excited state, a negative preexponential factor is expected at longer wavelengths where only the charge-transfer state emits. The results in diethyl ether and acetonitrile are not in accordance with this model of charge-transfer formation. In both solvents two decay times in the range of nanoseconds are observed. Moreover in acetonitrile the preexponential factors remain positive at longer wavelengths where only emission from a charge-separated state is expected. These results indicate the presence of two polar emitting species corresponding to two charge-transfer states, the πCT state, formed by transferring an electron to the benzonitrile part, and the σCT state, formed by transferring an electron to the monocyanoethylene part of the molecule.

Kinetic Analysis in Acetonitrile. Analysis of the fluorescence decay curves by means of global compartmental analysis renders information on the kinetics of the system in the excited state. From global analysis of the decay curves at different emission wavelengths, two emitting species can be distinguished and the system can be described as an intramolecular bicompartmental system. The identifiability problem for the intramolecular bicompartmental system has been extensively studied[56,57] and can be summarized as follows. If no fluorescence quencher is added to the system, three parameters have to be a priori known to extract all rate constants and spectral parameters from the fluorescence decay surface. For an intramolecular bicompartmental system in the presence of added fluorescence quencher, the fluorescence decay surface has to contain at least three different decay curves with three different quencher concentrations (of which one may be equal to 0) at the same excitation and emission wavelength. The rate constants of quenching of both compartments must differ. Only one system parameter, which may not be a rate constant for quenching, has to be known a priori. If no a priori information is available, upper and lower limits can be set on the rate constants through the so-called scanning technique. In this procedure, one parameter, for instance k_{01}, is kept constant at a preset value during analysis while the other parameters are freely adjustable, and the analysis is repeated for a range of preset values. A region can be defined for which each value of the scanned parameter results in a good fit. A plateau will be observed when S_1, S_2, and P (vide infra) are plotted as a function of the scanned parameter. Limits on the rate constants can be calculated using these parameters.

Theory. Consider an intramolecular system with two kinetically distinct species, two compartments, as given in Scheme 1. The rate constants of interest are k_{01} and k_{02}, the sums of the rate constants for all decay to the ground state for compartment 1* and 2*, respectively, k_{21} is the rate constant describing the transformation 1* → 2*, and k_{12} is the rate constant for the transformation from 2* → 1*. Addition of a fluorescence quencher Q accelerates the deactivation by k_{qi}[Q][i*]. It is assumed that the quencher does not alter the ground-state equilibrium and that the quenching is a Stern−Volmer type reaction.

The fluorescence decay after δ-pulse excitation can be written as a sum of two exponential functions:

$$f(\lambda^{em},\lambda^{ex},t) = \alpha_1 \exp(\gamma_1 t) + \alpha_2 \exp(\gamma_2 t) \quad (5)$$

The exponential factors γ_i are related to the observed decay times τ_i according to

$$\gamma_i = -1/\tau_i \quad (6)$$

Note that the exponential factors $\gamma_{1,2}$ depend exclusively on the rate constants and [Q].[58] The preexponential factors $\alpha_{1,2}$ depend on the rate constants, the quencher concentration [Q], the normalized absorbance $\tilde{b}_1(\lambda^{ex})$, and the normalized spectral emission weighting factors $\tilde{c}_1(\lambda^{em})$.[20] In the absence of any a priori information, the intervals of the rate constants k_{ij} can be determined by performing a series of global compartmental analyses in which one of the rate constants k_{ij} is kept constant at different preset values, while the remaining fitting parameters are freely adjustable (i.e., the "scanning" procedure). Keeping a rate constant fixed ensures that the system is identifiable in each of the analyses.[58−60] Using the estimated and preset values of the rate constants allows one to compute S_1, S_2, and P. with

$$S_1 = k_{01} + k_{21} \quad (7)$$

$$S_2 = k_{02} + k_{12} \quad (8)$$

$$P = k_{21}k_{12} \quad (9)$$

Plateaus will be observed when S_1, S_2, and P are plotted as a function of the scanned rate constant. The boundaries of the intervals for the rate constants are a function of S_1, S_2, and P[58] and are calculated using the average values for S_1, S_2, and P over the plateau region. The uncertainties on S_1, S_2, and P are calculated using the plateau limits.

TABLE 1: Fluorescence Decay Times of PCN2 in Acetonitrile with and without NaI Added

[Q]	τ_1 (ns)	τ_2 (ns)	$Z\chi_g^2$
0 M	2.8	11.2	0.07
0.001 M	2.8	9.9	1.29
0.01 M	2.3	5.2	1.5

The contribution of the excited-state species i^* to the total steady-state emission spectrum $F(\lambda^{em},\lambda^{ex})$ at emission wavelength λ^{em} due to excitation at λ^{ex} is called its species-associated emission spectrum, $\mathrm{SAEMS}_i(\lambda^{em},\lambda^{ex})$, and is given by[58]

$$\mathrm{SAEMS}_i(\lambda^{em},\lambda^{ex}) = \Omega_i(\lambda^{em},\lambda^{ex})\, F(\lambda^{em},\lambda^{ex}) \qquad (10)$$

where Ω_i, the emission weight factor, is a function of all the rate constants, the quencher concentration, the normalized absorbances, $\tilde{b}_i$, and the normalized emission weights, $\tilde{c}_i$.

If, and only if, $k_{12} = 0$ and $k_{21} = 0$, then[58,60]

$$\mathrm{DAS}_i(\lambda^{em},\lambda^{ex}) = f_i F(\lambda^{em},\lambda^{ex}) = \mathrm{SAEMS}_i(\lambda^{em},\lambda^{ex}) \quad (11)$$

where $\mathrm{DAS}_i(\lambda^{ex},\lambda^{em})$ is the decay-associated emission spectrum of species i^*,[61] with f_i the emission coefficient.

Global Compartmental Analysis for PCN2 in Acetonitrile. For the compound PCN2 in acetonitrile, no a priori information is assumed to be available. By means of global compartmental analysis using the scanning technique, upper and lower limits can be set on the rate constants. Fluorescence decay curves were measured without quencher added and with NaI added as a fluorescence quencher at two different quencher concentrations (0.001 M, 0.01 M). Measurements were performed with time increments of 98 and 49 ps at three emission wavelengths, 440, 480, and 520 nm. Another 11 decay curves at different wavelengths between 400 and 530 nm without quencher were added to the fluorescence surface. The decay curves at one quencher concentration were analyzed globally in terms of preexponential factors and decay times. In all cases a biexponential decay law could adequately describe the fluorescence decay surfaces. The decay times were found to be independent of the emission wavelength. The decay times at the different quencher concentrations are listed in Table 1. The preexponential factors depend on the emission wavelength and are all positive. The rate constants for quenching k_{q1} and k_{q2} are 10.5×10^9 L mol^{-1} s^{-1} and 13×10^9 L mol^{-1} s^{-1}, respectively.

All decay traces, 23 in total, were analyzed simultaneously by global compartmental analysis applying the scanning technique. The rate constant k_{01} was scanned in an interval between 0.001 and 0.5 ns^{-1} while leaving the other parameters freely adjustable. During the scanning, the parameters k_{01}, k_{02}, k_{21}, k_{12}, k_{q1}, k_{q2}, and $\tilde{b}_1$ were globally linked over the entire data surface, $\tilde{c}_1$ was linked over the quencher concentrations at equal emission wavelengths, while k_{q1} and k_{q2} were linked over experiments with added quencher. The resulting S_1, S_2, P, and $Z_{\chi_g}^2$ as a function of the scanned parameter k_{01} are graphically shown in Figure 5. The statistical parameter $Z_{\chi_g}^2$ is acceptable within a region limited by $k_{01} < 3.8 \times 10^8$ s^{-1}. For this same region average values for S_1, S_2, and P were calculated and are given in Table 2. The value for P is very small over the whole range of k_{01} values and approximates 0 at high k_{01} values. The average value for P over the region where $k_{01} < 3.8 \times 10^8$ s^{-1} is small, with a standard error of 100%. The upper and lower limits to the rate constants are calculated from the values of S_1, S_2, and P[58] and are compiled in Table 3. The value for $\tilde{b}_1$ differing from 1 or 0 indicates that both compartments are formed directly upon excitation.

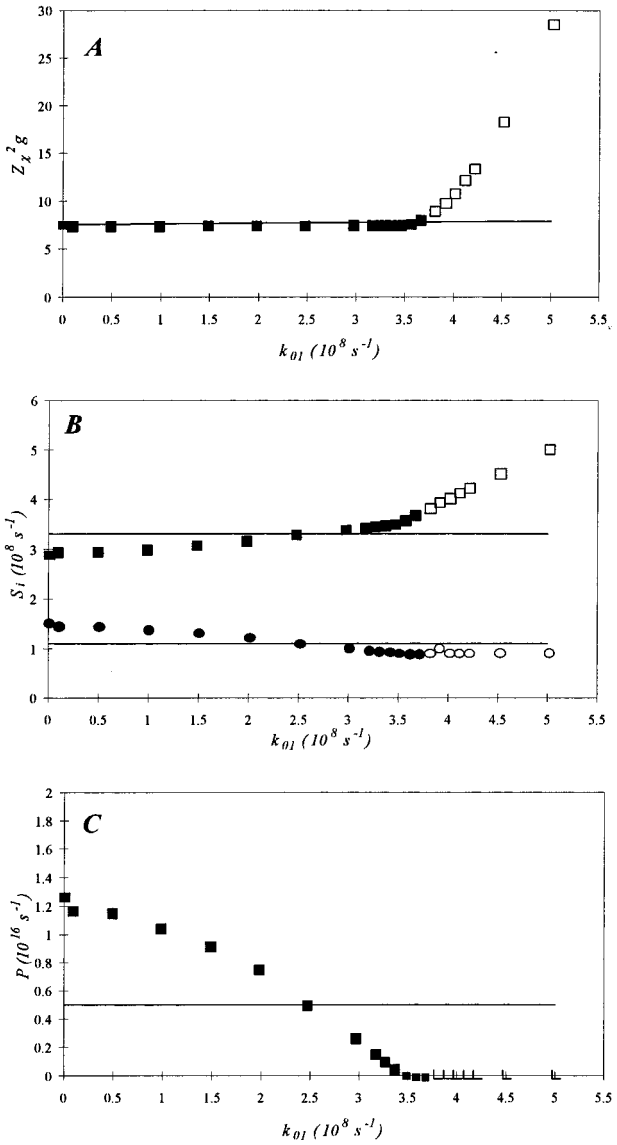

Figure 5. (A) $Z_{\chi_g}^2$, (B) (■) S_1 and (●) S_2, and (C) P from scanning k_{01} with all other parameters freely adjustable. Filled symbols represent the data used for calculating the mean values.

TABLE 2: Average S_1, S_2, and P Parameters and the Value $\tilde{b}_1$ Estimated by Combined Repetitive Global Compartmental Analyses from Scanning k_{01}

$S_1 = 3.3 \times 10^8 \pm 0.4 \times 10^8$ s^{-1}
$S_2 = 1.1 \times 10^8 \pm 0.3 \times 10^8$ s^{-1}
$P = 0.5 \times 10^{16} \pm 0.5 \times 10^{16}$ s^{-2}
$\tilde{b}_1 = 0.32 \pm 0.05$

TABLE 3: Calculated Upper and Lower Limits on the Rate Constants k_{01}, k_{21}, k_{02}, and k_{12}

0	<	k_{01} (10^8 s^{-1})	<	2.8 ± 1
0.5 ± 0.7	<	k_{21} (10^8 s^{-1})	<	3.3 ± 0.4
0	<	k_{02} (10^8 s^{-1})	<	0.9 ± 0.5
0.15 ± 0.17	<	k_{12} (10^8 s^{-1})	<	1.1 ± 0.3

As P is small, a value of P equal to 0 lies within the error of the value. In that case the system is irreversible in the excited state, and two kinetic models are possible, (i) (a) $k_{21} = 0$ or (b) $k_{12} = 0$, (ii) $k_{21} = 0$ and $k_{12} = 0$. Therefore k_{01} was scanned while k_{12} and/or k_{21} were kept constant at 0. In the case where k_{21} or k_{12} was kept equal to zero, good fits were acquired in the same intervals as when they were freely adjustable. Also keeping k_{21} and $k_{12} = 0$ resulted in a good fit. A differentiation between the two irreversible models can be made by comparing

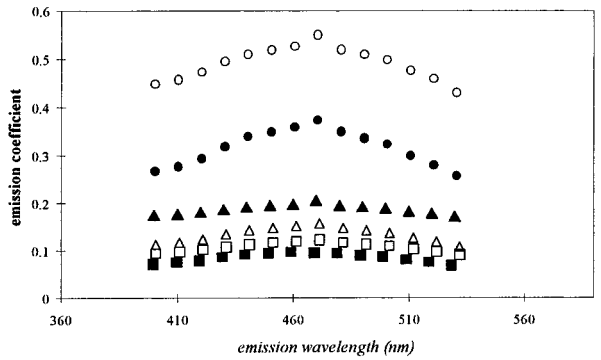

Figure 6. Values for the emission weight factor Ω_1 used for calculating the SAEMS of species 1 as a function of emission wavelength for (▲) $k_{12} = 0$ at $k_{01} = 0.001$; (□) $k_{12} = 0$ at $k_{01} = 0.3$; (●) $k_{21} = 0$ at $k_{02} = 0.001$; (△) $k_{21} = 0$ at $k_{02} = 0.08$; (○) $k_{21} = 0$ and $k_{12} = 0$ together with the emission coefficient f_1 (■) used for calculating the DAS of species 1.

the decay-associated spectra (DAS) with the species-associated emission spectra (SAEMS).[60] If k_{21} and k_{12} are both equal to zero, the DAS and SAEMS should be superimposable and all SAEMS calculated with the results of the different models at different values in the plateau should be identical. In all other cases the DAS and the SAEMS are different. It is easier, instead of comparing spectra, to compare the emission weight factors Ω_i; these are shown in Figure 6 for different values of k_{01} within the plateau together with the coefficient f_i for the DAS of species 1*. From this figure it is evident that the SAEMS are not unique and are different from the DAS, indicating that the kinetic model with $k_{21} = 0$ and $k_{12} = 0$ is not valid. The Ω_i values go through a maximum, indicating a severe overlap of the emission from the two compartments.

On the basis of global compartmental analysis one cannot distinguish between the models with $k_{21} = 0$ or $k_{12} = 0$. Moreover a value of $P = 0.5 \times 10^{16}$ s^{-2} implicates that one of the rate constants k_{21} or k_{12} does not necessarily has to be zero. Both rate constants could be on the order of 7×10^7 s^{-1}. Considering the magnitude of these values, they cannot be neglected with respect to the other rate constants, and one cannot state with certainty that one of the rate constants k_{21} or k_{12} is equal to 0.

Summarizing, this means that for the system PCN2 in acetonitrile, only upper limits can be set to the rate constants k_{12} and k_{21}, whereas one of these rate constants can be equal to zero but not both. Interconversion between the compartments in the excited state takes place at least in one direction with a rate constant $k_{21} < 3.3 \times 10^8$ s^{-1} and $k_{12} < 1.1 \times 10^8$ s^{-1}. The two compartments have an almost completely overlapping emission spectrum, indicating the emission of two polar species.

Discussion. From the single-photon-timing data and comparison with literature data for the model compounds it is clear that in the trichromophoric compound in medium and polar solvents, the electron is transferred in two directions. An electron is transferred from the amino part to the benzonitrile part to form a πCT state, and a σCT state is formed via through bond interaction of the donor and the second acceptor with the intervening σ-bonds. Emission from both polar charge-transfer states can be observed.

In acetonitrile, the contribution of the decay time remains positive at longer wavelengths and the emission weight factor Ω_i of the SAEMS indicates an important overlap of the emission from the two species. The rate constants for interconversion between the compartments are smaller than 3.3×10^8 s^{-1}. This interconversion is too slow to be attributed to a reaction from

SCHEME 2: Schematic Picture of the Excited-State Reaction of PCN2 in (a) Acetonitrile and (b) Diethyl Ether

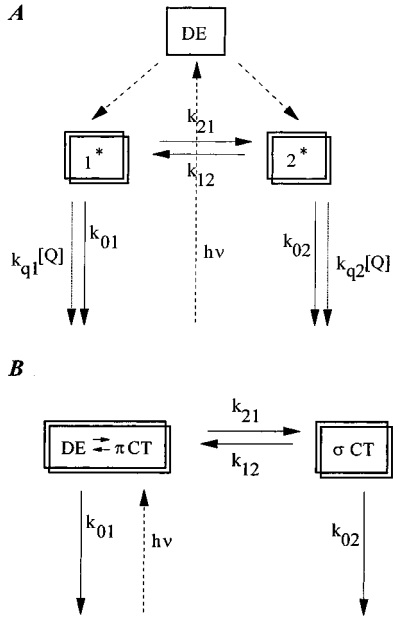

TABLE 4: Results of the Rate Constants for PCN2 in Acetonitrile Taking PIPBN as a Model Compound for the πCT State

compartment 1 the πCT state	compartment 2 the σCT state
$k_{01} = 2.8 \times 10^8$ s^{-1}	$k_{02} = 0.1 \times 10^8$ s^{-1}
$k_{21} = 0.5 \times 10^8$ s^{-1}	$k_{12} = 1 \times 10^8$ s^{-1}

an initially excited state to a CT state whether this is the σCT or πCT state. Therefore, and taking into account the strong overlap in emission, we attribute the two compartments to two CT states, the σCT and πCT state. As the initially excited state cannot be kinetically distinguished and as the driving force for formation of the CT states from the initially excited state is large in a polar solvent like acetonitrile, we assume in a first approximation that the initially excited state (DE) can be regarded as the excitation source, as given in Scheme 2a. This correlates with the steady-state emission spectrum where in acetonitrile emission from the polar states dominates. A parameter $\tilde{b}_1$ differing from 1 or 0 indicates that both charge-transfer states are formed directly upon excitation, from the initially excited state.

The compound MOD2 cannot be regarded as a good model compound for the kinetic analysis due to the difference in donor strength. The model compound PIPBN is also not a real model compound as it is already a bicompartmental system itself. However we can assume that the decay time of 3.6 ns for PIPBN in acetonitrile is determined mainly by emission of the charge-transfer state. In that case the rate constant for decay of the πCT state of PCN2 given by k_{0i}, is equal to 2.8×10^8 s^{-1} ($1/\tau_{\text{PIPBN}}$). This extra information can be used to determine the other rate constants. In theory, there are still two sets of rate constants possible, as the compartments are interchangeable. For PCN2 in acetonitrile, the value of the rate constant of the model compound fits only within the interval of compartment 1. Compartment 1 can be assigned to the πCT state and compartment 2 to the σCT state. The results for the rate constants are given in Table 4.

The results indicate that the rate constant for formation of the πCT state from the σCT state has an upper limit of $1.1 \times$

10^8 s^{-1}. During this excited-state reaction, a negative charge is transferred from one end of the molecule to the other. The large solvent reorganization that accompanies the reaction results in a large activation energy for electron transfer. The rate of electron transfer is given by

$$k_{et} = k_0 \exp\left[-\frac{(\Delta G^\circ + \lambda)^2}{4\lambda kT}\right] \quad (12)$$

k_0 is the maximum rate of reaction in absence of activation energy, k is the Boltzmann constant, and T is the temperature. λ denotes the reorganization energy dominated by the solvent reorganization, which is given by

$$\lambda_s = \frac{e^2}{4\pi\epsilon_0}\left(\frac{1}{r} - \frac{1}{R_c}\right)\left(\frac{1}{n^2} - \frac{1}{\epsilon_s}\right) \quad (13)$$

If the rate of reaction in the absence of the activation energy is assumed equal to 1×10^{13} s^{-1} and if the driving force of the reaction is equal to zero, the reorganization energy must be smaller than 1.18 eV to obtain a rate constant of 1×10^8 s^{-1}. This means that for a distance of 8 Å between the chromophores, the radius of the chromophores should be at least 3.5 Å which is an acceptable value. These calculations demonstrate that with a solvent reorganization energy needed to transfer a negative charge over a distance of 8 Å a rate constant of 1×10^8 s^{-1} can still be obtained. A contribution of the intramolecular reorganization will lead to smaller rate constants. When there is driving force for the reaction, the same rate constant can be obtained for a higher reorganization energy.

If in diethyl ether only one CT state would be formed, independently of whether this is the σCT or the πCT state, we would expect, on the basis of the data for the model compounds, a biexponential decay with one very short decay time (in the picosecond range) indicating a fast formation of the charge-transfer state from the initially excited state. This decay time might even possibly be too small to be observed within the time resolution of the experimental setup. In diethyl ether, two decay times in the range of nanoseconds are observed, which is not in accordance with the model of formation of only one CT state. The contribution of the short decay time becomes negative at longer wavelengths and the ratio of the preexponential factors approaches -1 at long wavelengths. This indicates that only one compartment is formed directly upon excitation. After formation of this first compartment, the second compartment is formed through an excited-state reaction. The emission spectrum consists of both charge-transfer emission and emission from the initially excited state. Furthermore we can assume that for the model compound PIPBN in diethyl ether, where dual emission is observed, the interconversion between the initially excited state and charge-transfer state is very fast such that the two species cannot be distinguished kinetically. Therefore, in the trichromophoric system in diethyl ether, the first compartment can approximately be attributed to the initially excited and πCT state, two species that kinetically cannot be distinguished, whereas the second compartment can be attributed to the σCT state (Scheme 2b).

Acknowledgment. The continuous support of the Ministry of Science Programming through IUAP 4-11 is gratefully acknowledged. S.D. thanks the KU Leuven and the IWONL for financial support. N. Boens (KU Leuven) is thanked for the development of the algorithms for the analysis of the "single-photon-timing" analysis and global compartmental analysis. M. Van der Auweraer and J. van Stam (KU Leuven) are thanked for fruitful discussions.

References and Notes

(1) Wasielewski, M. R. *Chem. Rev.* **1992**, *92*, 435.
(2) Gust, D.; Moore, T. A.; Moore, A. L. *Acc. Chem. Res.* **1993**, *26*, 198.
(3) Sauvage, J. P.; Collin, J. P.; Chambron, J. C.; Guillerez, S.; Coudret, C.; Balzani, V.; Barigelletti, F.; De Cola, L.; Flamigni, L. *Chem. Rev.* **1994**, *94*, 993.
(4) Maruyama K.; Osuka, A.; Mataga, N. *Pure Appl. Chem.* **1994**, *66*, 867.
(5) (a) Gust, D.; Moore, T. A.; Moore, A. L.; Barrett, D.; Harding, L. O.; Makings, L. R.; Liddell, P. A.; De Schryver, F. C.; Van der Auweraer, M.; Bensasson, R. V.; Rougée, M. *J. Am. Chem. Soc.* **1988**, *110*, 321. (b) Lee, S.-J.; De Graziano, J. M.; Mac Pherson, A. N.; Shin, E.-J.; Kerrigan, P. K.; Seely, G. R.; Moore, A. L.; Moore, T. A.; Gust, D. *Chem. Phys.* **1993**, *176*, 321.
(6) Gust, D.; Moore, T. A.; Moore, A. L.; Mac Pherson, A. N.; Lopez, A.; De Graziano, J. M.; Gouni, I.; Bittersmann, E.; Seely, G. R.; Gao, F.; Nieman, R. A.; Ma, X. C.; Demanche, L. J.; Hung, S.-C.; Luttrull, D. K.; Lee, S.-J.; Kerrigan, P. K. *J. Am. Chem. Soc.* **1993**, *115*, 11141.
(7) Brouwer, A. M.; Eijckelhoff, C.; Willemse, R. J.; Verhoeven, J. W.; Schuddeboom, W.; Warman, J. M. *J. Am. Chem. Soc.* **1993**, *115*, 2988.
(8) Willemse, R. J.; Verhoeven, J. W.; Brouwer, A. M. *J. Phys. Chem.* **1995**, *99*, 5753.
(9) Greenfield, S. R.; Svec, W. A.; Gosztola, D.; Wasielewski, M. R. *J. Am. Chem. Soc.* **1996**, *118*, 6767.
(10) Osuka, A.; Marumo, S.; Mataga, N.; Tanaguchi, S.; Okada, T.; Yamazaki, I.; Nishimura, Y.; Ohno, T.; Nozaki, K. *J. Am. Chem. Soc.* **1996**, *118*, 155.
(11) Van Dijk, S. I.; Wiering, P. G.; Groen, C. P.; Brouwer, A. M.; Verhoeven, J. W.; Schuddeboom, W.; Warman, J. M. *J. Chem. Soc., Faraday Trans.* **1995**, *91*, 2107.
(12) Roest, M. R.; Verhoeven, J. W.; Schuddeboom, W.; Warman, J. M.; Lawson, J. M.; Paddon-Row, M. N. *J. Am. Chem. Soc.* **1996**, *118*, 1762.
(13) De Schryver, F. C.; Declercq, D.; Depaemelaere, S.; Hermans, E.; Onkelinx, A.; Verhoeven, J. W.; Gelan, J. *J. Photochem. Photobiol. A: Chem.* **1994**, *82*, 171.
(14) Taylor, S. *Synthesis* **1981**, *8*, 606.
(15) Hermant, R. M.; Bakker, N. A. C.; Scherer, T.; Krijnen, B.; Verhoeven, J. W. *J. Am. Chem. Soc.* **1990**, *112*, 1214.
(16) Khalil, M. M. H.; Boens, N.; Van der Auweraer, M.; Ameloot, M.; Andriessen, R.; Hofkens, J.; De Schryver, F. C. *J. Phys. Chem.* **1991**, *95*, 9375.
(17) Boens, N. *Luminescence techniques in chemical and biochemical analysis*; Dekker: New York, 1991; p 21.
(18) Boens, N.; Ameloot, M.; Yamazaki, I.; De Schryver, F. C. *Chem. Phys.* **1988**, *121*, 73.
(19) Boens, N.; Janssens, L.; Ameloot, M.; De Schryver, F. C. *Proc. SPIE Conf., Time Resolved Laser Spectroscopy in Biochemistry II*; Los Angeles, SPIE 1990; p 456.
(20) Ameloot, M.; Boens, N.; Andriessen, E.; Van den Bergh, V.; De Schryver, F. C. *J. Phys. Chem.* **1991**, *95*, 2041.
(21) Andriessen, R.; Boens, N.; Ameloot, M.; De Schryver, F. C. *J. Phys. Chem.* **1991**, *95*, 2048.
(22) Boens, N.; Janssens, L. D.; De Schryver, F. C. *Biophys.Chem.* **1989**, *33*, 77.
(23) Van den Zegel, M.; Boens, N.; Daems, D.; De Schryver, F. C. *Chem. Phys.* **1986**, *101*, 311.
(24) Lippert, E.; Lüder, W.; Moll, F.; Nagele, H.; Boos, H.; Prigge, H.; Siebold-Blankenstein, I. *Angew. Chem.* **1961**, *73*, 695.
(25) Lippert, E.; Lüder, W.; Boos, H. *Advances in molecular spectroscopy*; Mangini, A., Ed.; 1962; p 443.
(26) Rettig, W. *Proc. Indian Acad. Sci. (Chem. Sci.)* **1992**, *104*, 89.
(27) Rettig, W. *Top. Curr. Chem.* **1994**, *169*, 254.
(28) Rotkiewicz, K.; Grellmann, K. H.; Grabowski, Z. R. *Chem. Phys. Lett.* **1973**, *19*, 315.
(29) Rotkiewicz, K.; Grabowski, Z. R.; Krowczynski, A.; Kühnle, W. *J. Lumin.* **1976**, *12*, 877.
(30) Grabowski, Z. R.; Rotkiewicz, K.; Siemiarczuk, A.; Cowley, D. J.; Baumann, W. *Nouv. J. Chim.* **1979**, *3*, 443.
(31) Grabowski, Z. R.; Rotkiewicz, K.; Rubaszewska, W.; Kirkor-Kaminska, E. *Acta Phys. Pol., A* **1978**, *54*, 767.
(32) Grabowski, Z. R.; Rotkiewicz, K.; Siemiarczuk, A. *J. Lumin.* **1979**, *18*, 420.
(33) Rettig, W. *J. Phys. Chem.* **1982**, *86*, 1970.
(34) Rullière, C.; Grabowski, Z. R.; Dobkowski, J. *Chem. Phys. Lett.* **1987**, *137*, 408.
(35) Okada, T.; Mataga, N.; Baumann, W. *J. Phys. Chem.* **1987**, *91*, 760.

(36) Serrano-Andrés, L.; Merchán, M.; Roos, B. O.; Lindh, R. *J. Am. Chem. Soc.* **1995**, *117*, 3189.
(37) Gorse, A.-D.; Pesquer, M. *J. Phys. Chem.* **1995**, *99*, 4039.
(38) Broo, A.; Zerner, M. C. *Theor. Chim. Acta* **1995**, *90*, 383.
(39) Soujanya, T.; Saroja, G.; Samanta, A. *Chem. Phys. Lett.* **1995**, *236*, 503.
(40) Schuddeboom, W.; Jonker, S. A.; Warman, J. M.; Leinhos, U.; Kühnle, W.; Zachariasse, K. A. *J. Phys. Chem.* **1992**, *96*, 10809.
(41) Leinhos, U.; Kühnle, W.; Zachariasse, K. A. *J. Phys. Chem.* **1991**, *95*, 2013.
(42) Zachariasse, K. A.; Grobys, M.; von der Haar, Th.; Hebecker, A.; Il'Ichev, Y.; Kühnle, W.; Morawski, O. *J. Inf. Rec.* **1996**, *22*, 553.
(43) Zachariasse, K. A.; von der Haar, Th.; Leinhos, U.; Kühnle, W. *J. Inf. Rec. Mater.* **1994**, *21*, 501.
(44) Zachariasse, K. A.; von der Haar, Th.; Hebecker, A.; Leinhos, U.; Kühnle, W. *Pure Appl. Chem.* **1993**, *65*, 1745.
(45) Rettig, W. *Ber. Bunsen-Ges. Phys. Chem.* **1991**, *95*, 259.
(46) Braun, D.; Rettig, W. *Chem. Phys.* **1994**, *180*, 231.
(47) Fisz, J. *J. Chem. Phys.* **1995**, *192*, 163.
(48) Zachariasse, K. A.; von der Haar, Th.; Leinhos, U.; Kühnle, W. *J. Inf. Rec. Mater.* **1994**, *21*, 501.9.
(49) Zachariasse, K. A.; Grobys, M.; von der Haar, Th.; Hebecker, A.; Il'Ichev, Yu. V.; Jiang, Y. B.; Morawski, O.; Kühnle, W. *J. Photochem. Photobiol. A: Chem.* **1996**, *102*, 59−70.
(50) Lippert, E. *Z. Naturforsch. A* **1955**, *10*, 541.
(51) Lippert, E. *Ber. Bunsen-Ges. Phys. Chem. (Z. Electrochem.)* **1957**, *61*, 962.
(52) Mataga, N.; Kaifu, Y.; Koizumi, M. *Bull. Chem. Soc. Jpn.* **1956**, *29*, 465.
(53) Liptay, W. In *Excited States*; Lim, E. C., Ed.; Academic Press: New York, 1974; p 129.
(54) Baumann, W.; Nagy, Z.; Maiti, A. K.; Reis, H.; Rodriges, S. V.; Detzer, N. *Yamada Conference XXIX on Dynamics and Mechanism of Photoinduced Electron Transfer and Related Phenomena*, Osaka, Japan; Mataga, N., Okada, N., Masuhara, H., Eds.; Elsevier: Amsterdam, 1992; p 211.
(55) Onsager, L. *J. Am. Chem. Soc.* **1936**, *58*, 1486.
(56) Boens, N.; Ameloot, M.; Hermans, B.; De Schryver, F. C.; Andriessen, R. *J. Phys. Chem.* **1993**, *97*, 799.
(57) Hermans, B. Ph.D. Dissertation, K.U. Leuven, 1994.
(58) Van Dommelen, L.; Boens, N.; Ameloot, M.; De Schryver, F. C.; Kowalczyck, A. *J. Phys. Chem.* **1993**, *97*, 11738.
(59) Van Dommelen, L.; Boens, N.; Ameloot, M.; De Schryver, F. C.; Kowalczyk, A. *J. Phys. Chem.* **1993**, *97*, 799.
(60) Van Dommelen, L.; Boens, N.; De Schryver, F. C.; Ameloot, M. *J. Phys. Chem.* **1995**, *99*, 8959.
(61) Wahl, Ph.; Auchet, J. C. *Biochem. Biophys. Acta* **1972**, *285*, 99.